Plasphonics : local hybridization of plasmons and phonons

Renaud Marty, Adnen Mlayah, Arnaud Arbouet, Christian Girard, Sudhiranjan Tripathy

Plasphonics : local hybridization of plasmons and phonons

Renaud Marty,[1,2] Adnen Mlayah,[1,2,*] Arnaud Arbouet,[1,2] Christian Girard,[1,2] and Sudhiranjan Tripathy[3]

[1] *CNRS, CEMES (Centre dElaboration des Materiaux et dEtudes Structurales), BP 94347, 29 rue J. Marvig, F-31055 Toulouse, France* [2] *Universite de Toulouse, UPS, 29 rue J. Marvig, F-31055, Toulouse, France* [3] *Institute of Materials Research and Engineering, Agency for Science, Technology, and Research, 3 Research Link, 117602 Singapore*

[*]*adnen.mlayah@cemes.fr*

Abstract: We show that the interaction between localized surface plasmons sustained by a metallic nano-antenna and delocalized phonons lying at the surface of an heteropolar semiconductor can generate a new class of hybrid electromagnetic modes. These *plasphonic modes* are investigated using an analytical model completed by accurate Green dyadic numerical simulations. When surface plasmon and surface phonon frequencies match, the optical resonances exhibit a large Rabi splitting typical of strongly interacting two-level systems. Based on numerical simulations of the electric near-field maps, we investigate the nature of the plaphonic excitations. In particular, we point out a strong local field enhancement boosted by the phononic surface. This effect is interpreted in terms of light harvesting by the plasmonic antenna from the phononic surface. We thus introduce the concept of *active phononic surfaces* that may be exploited for far-infared optoelectronic devices and sensors.

© 2013 Optical Society of America

OCIS codes: (240.0240) Optics at surfaces; (300.0300) Spectroscopy.

References and links

1. C. F. Bohren and D. R. Huffman, *Absorption and Scattering of Light by Small Particles* (New York Wiley-Interscience, 1983).
2. L. Novotny and B. Hecht, *Principles of Nano-Optics* (Cambridge U. Press New York, 2006).
3. H. A. Atwater and A. Polman, "Plasmonics for improved photovoltaic devices," Nat. Mater. **9**, 205–213 (2010).
4. S. Lal, S. Link and N. J. Halas, "Nano-optics from sensing to waveguiding," Nat. Photonics **1**, 641–648 (2007).
5. R. Hillenbrand, T. Taubner, and F. Keilmann, "Phonon-enhanced light-matter interaction at the nanometre scale," Nature **418**, 159–162 (2002).
6. M. S. Anderson, "Surface enhanced infrared absorption by coupling phonon and plasmon resonance," Appl. Phys. Lett. **87**, 144102 (2005).
7. F. Neubrech, A. Pucci, T. W. Cornelius, S. Karim, A. Garcia-Etxarri, and J. Aizpurua, "Resonant plasmonic and vibrational coupling in a tailored nanoantenna for infrared detection," Phys. Rev. Lett. **101**, 157403 (2008).
8. H. Wang, D. W. Brandl, F. Le, P. Nordlander, and N. J. Halas, "Nanorice: a hybrid plasmonic nanostructure," Nano Lett. **6**, 827–832 (2006).
9. G. A. Wurtz, P. R. Evans, W. Hendren, R. Atkinson, W. Dickson, R. J. Pollard, A. V. Zayats, W. Harrison, and C. Bower, "Molecular plasmonics with tunable exciton-plasmon coupling strength in J-aggregate hybridized Au nanorod assemblies," Nano Lett. **7**, 1297–1303 (2007).
10. N. T. Fofang, T. H. Park, O. Neumann, N. A. Mirin, P. Nordlander, and N. J. Halas, "Plexcitonic nanoparticles: plasmon-exciton coupling in nanoshell-J-aggregate complexes," Nano Lett. **8**, 3481–3487 (2008).
11. S. Savasta, R. Saija, A. Ridolfo, O. Di Stefano, P. Denti, and F. Borghese, "Nanopolaritons: vacuum rabi splitting with a single quantum dot in the center of a dimer nanoantenna," ACS Nano **4**, 6369–6376 (2010).

12. A. Manjavacas, F. G. de Abajo, and P. Nordlander, "Quantum plexcitonics: strongly interacting plasmons and excitons," Nano Lett. **11**, 2318–2323 (2011).
13. S. Grabowski, T. Kampen, H. Nienhaus, and W. Monch, "Vibrational properties of GaN(0001) surfaces," Appl. Surf. Sci. **123**, 33–37 (1998).
14. N. Esser and W. Richter, *Raman Scattering from Surface Phonons* (Springer Berlin / Heidelberg, 96–168, 2000).
15. A. Mooradian and G. B. Wright, "Observation of the interaction of plasmons with longitudinal optical phonons in GaAs," Phys. Rev. Lett. **16**, 999–1001 (1966).
16. M. Abstreiter, G. Cardona, and A. Pinczuk, *Light Scattering by Free Carrier Excitations in Semiconductors* (Springer-Verlag, Berlin, 1984).
17. A. Huber, N. Ocelic, T. Taubner, and R. Hillenbrand, "Nanoscale resolved infrared probing of crystal structure and of plasmon-phonon coupling," Nano Lett. **6**, 774–778 (2006).
18. H. C. Kim and X. Cheng, "Infrared dipole antenna enhanced by surface phonon polaritons," Opt. Lett. **35**, 3748–3750 (2010).
19. G. Yu, N. L. Rowell, and D. J. Lockwood, "Anisotropic infrared optical properties of GaN and sapphire," J. Vac. Sci. Technol. A **22**, 1110–1114 (2004).
20. D. Lockwood, G. Yu, and N. L. Rowell, "Optical phonon frequencies and damping in AlAs, GaP, GaAs, InP, InAs and InSb studied by oblique incidence infrared spectroscopy," Solid State Commun. **136**, 404–409 (2005).
21. L. Novotny, "Effective wavelength scaling for optical antennas," Phys. Rev. Lett. **98**, 266802 (2007).
22. H. Wei, A. Reyes-Coronado, P. Nordlander, J. Aizpurua, and H. Xu, "Multipolar plasmon resonances in individual Ag nanorice," ACS Nano **4**, 2649–2654 (2010).
23. B. S. Guiton, V. Iberi, S. Li, D. N. Leonard, C. M. Parish, P. G. Kotula, M. Varela, G. C. Schatz, S. J. Pennycook, and J. P. Camden, "Correlated optical measurements and plasmon mapping of silver nanorods," Nano Lett. 11, 3482–3488 (2011).
24. C. Girard , "Near field in nanostructures," Rep. Prog. Phys. **68** 1883-1933 (2005)
25. O. Keller, M. Xiao, and S. Bozhevolnyi, "Configurational resonances in optical near-field microscopy: a rigorous point-dipole approach," Surf. Sci. **280**, 217–230 (1993).
26. J. Dintinger, S. Klein, F. Bustos, W. L. Barnes, and T. W. Ebbesen, "Strong coupling between surface plasmon-polaritons and organic molecules in subwavelength hole arrays," Phys. Rev. B **71**, 035424 (2005).
27. L. Novotny, "Strong coupling, energy splitting, and level crossings: a classical perspective," Am. J. Phys. **78**, 1199–1202 (2010).
28. O. J. F. Martin, C. Girard and A. Dereux, "Generalized field propagator for electromagnetic scattering and light confinement," Phys. Rev. Lett. **74**, 526 (1995).
29. D. Barchiesi, C. Girard, O. J. F. Martin, D. Van Labeke, and D. Courjon, "Computing the optical near-field distributions around complex subwavelength surface structures: a comparative study of different methods," Phys. Rev. E **54** 4285–4292 (1996).
30. M. A. Ordal, L. L. Long, R. J. Bell, S. E. Bell, R. W. Bell, J. Alexander, and C. A. Ward, "Optical properties of the metals Al, Co, Cu, Au, Fe, Pb, Ni, Pd, Pt, Ag, Ti, and W in the infrared and far infrared," Appl. Opt. **22**, 1099–1119 (1983).
31. S. Aksu, A. A. Yanik, R. Adato, A. Artar, M. Huang, and H. Altug, "High-throughput nanofabrication of infrared plasmonic nanoantenna arrays for vibrational nanospectroscopy," Nano Lett. **10**, 2511–2518 (2010).
32. E. Cubukcu, E. A. Kort, K. B. Crozier, and F. Capasso, "Plasmonic laser antenna," Appl. Phys. Lett. **89**, 093120 (2006).

---

1. Introduction

Over the last twenty years, a considerable amount of original nano–photonic developments were based on the mastering of the physics of surface plasmons. For example, the well–known tunability of the optical response of plasmonic particles [1] or lithographically designed metallic nanostructures have generated numerous applications in integrated optics, biosensing, nanomedicine and photovoltaics [2–4]. Recently it has been shown that plasmonic based applications could strongly benefit from the hybridization of surface plasmons and phonons [5–7] or excitons [8–12].

Surface plasmon resonances occur when the real part of the metal permittivity takes negative values. Similarly, a dielectric material can also exhibit a metallic behavior provided its dielectric constant is negative in a given frequency domain. In the case of polar semiconductors, this occurs in the Reststrahllen band, *i.e.* between the transverse and the longitudinal optical phonon frequencies. In this frequency gap, the atomic vibrations generate electromagnetic fields that propagate along the surface with a strong localization in the perpendicular direction. These

modes have been extensively studied by high resolution electron energy loss spectroscopy [13] and Raman scattering [14].

Hybridization between phonons and plasmons has been reported earlier by Mooradian and Wright [15] and was investigated in a variety of doped bulk semiconductors [16]. More recently, Neubrecht *et al* [7] have observed a Fano type resonance when molecular vibrations are coupled to far infrared surface plasmons. Using infrared near-field optical microscopy, Hillenbrand et al. [5] have observed the surface plasmon-surface phonon hybridization and Anderson [6] has pointed out the interest of such hybridization for enhanced infrared spectroscopy. In a similar context, Huber *et al* [17] have demonstrated the generation and focusing of surface phonon–polaritons at the surface of a SiC crystal by using elongated metal nanostructures. Following these experiments, preliminary theoretical studies have highlighted the strong concentration of infrared energy that are produced by the synergistic interaction of surface plasmons and surface phonons [18].

In this Letter, we consider the strong interaction regime between the surface plasmons sustained by a gold nano–antenna and surface phonons of a polar substrate. In particular, we investigate the transition between strong and weak coupling regimes and show that Rabi–type splitting and mixing between surface plasmons and surface phonons occurs. In a first step, the physics of the interaction between plasmonic and phononic excitations is analyzed from purely analytical descriptions of the optical responses. Within the limit of the applicability of such a model, it is possible to bring to the fore the main physical mechanisms and parameters responsible for this interaction. The analytical results are then completed by realistic Green dyadic numerical simulations of the optical resonances and the corresponding electric near–field maps.

2. Analytical approach

We consider the dielectric response of a polar semiconductor in the optical phonon frequency range. Depending on the crystal structure, several phonon branches may contribute to the dielectric function and could therefore interact with surface plasmons [19, 20]. For the sake of simplification, we introduce only the phonon branches which generate electric field parallel to the crystal surface and is therefore able to couple to the longitudinal surface plasmons of the nano–antenna. For instance, in the case of wurtzite GaN with c-axis perpendicular to the surface, this corresponds to the longitudinal $E_1(LO)$ and transverse $E_1(TO)$ phonons. Let ω_L, ω_T and γ_L, γ_T be respectively the $E_1(LO)$ and $E_1(TO)$ optical phonon frequencies and their corresponding damping parameters, the dielectric function reads [19, 20]

$$\varepsilon(\omega) = \varepsilon_\infty \frac{\omega_L^2 - \omega^2 + i\omega\gamma_L}{\omega_T^2 - \omega^2 + i\omega\gamma_T} \tag{1}$$

In the following, GaN has been chosen for its quite large LO-TO splitting. The phonon frequencies, the damping parameters and the high frequency dielectric constant ε_∞ are taken from reference [19]. However, the results reported in this work are quite general and could be extended to other polar semiconductors (SiC, GaAs...).

For an air-exposed two-dimensional surface, the electromagnetic boundary conditions are fulfilled for $\varepsilon(\omega) = -1$ in the long-wavelength limit. Since the LO and TO phonon dampings are much smaller than the LO and TO frequencies [19, 20], the γ_L and γ_T terms in Eq. (1) can be neglected and using $\varepsilon(\omega) = -1$, one obtains the surface phonon frequency $\omega_{sph}^2 = (\omega_T^2 + \varepsilon_\infty\omega_L^2)/(1 + \varepsilon_\infty)$ which falls in the LO-TO Reststrahllen gap. On the other hand, the surface plasmons of a metallic nano–antenna can be tuned from the visible to the far infrared spectral region by increasing the length/width aspect ratio [7, 21, 23]. It is thus possible to tune the surface plasmon frequency close to the surface phonon frequency by changing the aspect ratio
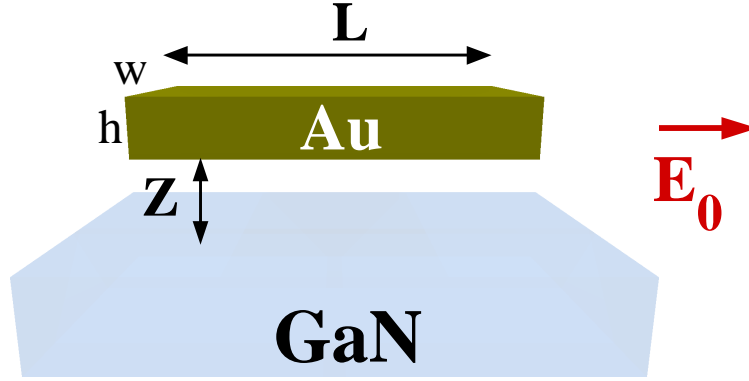
Fig. 1. Schematic of the system studied in this work. A gold antenna (length L, width w=200 nm, height h=100 nm) is located in the vicinity of a polar semiconductor GaN surface. The system is illuminated at normal incidence by an incident electric field $\mathbf{E}_0$ oscillating at frequency ω and parallel to the long axis of the metallic antenna.

of a plasmonic antenna. This remarkable property can be used to match surface plasmon and surface phonon frequencies.

The system studied in this work consists in a single gold antenna separated from the surface of a polar semiconductor by an air gap (Fig. 1). In order to excite the longitudinal surface plasmons, the system is illuminated at normal incidence by a monochromatic electric field parallel to the antenna long axis. For a very long antenna, the longitudinal surface plasmon frequencies ω_p only depend on the antenna length L [21]. In this case $\omega_p = c\pi p/nL$, where p is an integer that labels the surface plasmon mode order, n is the effective optical index of the environment surrounding the antenna [21, 22] and c is the speed of light. The fundamental mode $p = 1$ corresponds to a dipolar distribution of the electric field with surface polarization charges located at both antenna ends [23]. To keep within analytical and tractable calculations, we assume that the antenna is excited on its fundamental mode, and thus behaves as an induced point dipole located at the antenna center $\mathbf{R} = (0, 0, R = Z + h/2)$ (Z being the width of the air-gap and h the height of the antenna (Fig. 1)). Its polarizability is described by a lorentzian function

$$\alpha(\omega) = \alpha_0 \frac{\omega_1^2}{\omega_1^2 - \omega^2 + i\omega\gamma_1} \tag{2}$$

where $\omega_1 = c\pi/nL$ is the resonance frequency, γ_1 is a damping parameter and α_0 is a static polarizability fixed to its maximum value, i.e. to the antenna volume (in CGS units). In the framework of the field susceptibility formalism [24], the electric field at the dipole location is given by [25]

$$\mathbf{E}(\mathbf{R}, \omega) = [\mathbf{I} - \alpha(\omega) \cdot \mathbf{S}(\mathbf{R}, \omega)]^{-1} \cdot \mathbf{E}_0(\mathbf{R}, \omega) \tag{3}$$

where the dyadic tensor $\mathbf{S}$ represents the field-susceptibility of the surface, $\mathbf{I}$ is the identity tensor, and $\mathbf{E}_0(\mathbf{R}, \omega)$ is the incident electric field. The wavelengths of the surface plasmons considered here are of the order of 20 μm, i.e. much larger than the spacing Z (few tens of nanometers) between the dipole antenna and the semiconductor surface. In that case, the dipole-surface interaction is described by the near-field contribution to $\mathbf{S}$ [25]

$$\mathbf{S}(\mathbf{R}, \omega) = \frac{\varepsilon(\omega) - 1}{\varepsilon(\omega) + 1} \cdot \frac{1}{R^3} \cdot \begin{pmatrix} 1 & 0 & 0 \\ 0 & 1 & 0 \\ 0 & 0 & 2 \end{pmatrix} \tag{4}$$

Using Eqs. (3)-(4), one derives the overall electric field and the induced dipole which, for an incident polarization parallel to the antenna, reads

$$\mathbf{p}(\mathbf{R},\omega) = \frac{\alpha(\omega)}{1 - \frac{1}{(2R)^3}\frac{\varepsilon(\omega)-1}{\varepsilon(\omega)+1}\alpha(\omega)} \cdot \mathbf{E}_0(\mathbf{R},\omega) \tag{5}$$

The induced dipole clearly depends on the distance between the antenna and the heteropolar semiconductor surface through the $1/R^3$ term. For negligible surface plasmon and surface phonon dampings, resonances occur for frequencies satisfying

$$\Re\{1 - \frac{1}{(2R)^3}\frac{\varepsilon(\omega)-1}{\varepsilon(\omega)+1}\alpha(\omega)\} = 0 \tag{6}$$

where $\Re$ denotes the real part. Replacing Eqs. (1)-(2) into Eq. (6) leads to the bi–squared equation

$$0 = (\omega^2 - \omega_{SP}^2(Z))(\omega^2 - \omega_{sph}^2) - \delta^2 \frac{\omega_1^2 \varepsilon_\infty^2}{(\varepsilon_\infty+1)^2}\frac{\alpha_0}{4(Z+h/2)^3} \tag{7}$$

where $\delta^2 = \omega_L^2 - \omega_T^2$, and $\omega_{SP}^2(Z) = \omega_1^2(1 + \frac{\alpha_0}{8(Z+h/2)^3}\frac{\varepsilon_\infty-1}{\varepsilon_\infty+1})$ is the dipole–antenna resonance frequency modified by the Z–dependent dipole image effect. The last term of Eq. (7) accounts for the interaction between the surface phonons and the dipole–antenna. For a non polar semiconductor, there is no electromagnetic field generated by the surface phonons. In that case, $\delta = 0$ in Eq. (7) gives *two independent solutions* ω_{sph} and $\omega_{SP}(Z)$. Conversely, for $\delta \neq 0$, the coupling between the surface phonons and the dipole-antenna resonance can occur. The two real solutions ω_+ and ω_- of Eq. (7) are plotted in Fig. 2(a) as a function of the dipole antenna resonance frequency ω_1 and for different dipole–to–surface separations. By changing ω_1, the surface plasmon frequency $\omega_{SP}(Z)$ can be tuned to the surface phonon frequency ω_{sph} and an anti–crossing typical of Rabi–splitted two–level systems is observed [26, 27]. This behavior is the signature of the strong coupling between the dipole-antenna and the surface phonons. Using the resonance condition $\omega_{SP}(Z) = \omega_{sph}$ and $\delta << \omega_{sph}$ in Eq. (7), one obtains the Rabi splitting Δ

$$\Delta = \omega_+ - \omega_- = \delta \cdot \frac{\omega_1}{\omega_{sph}} \cdot \frac{\varepsilon_\infty}{\varepsilon_\infty+1} \cdot \frac{\alpha_0^{1/2}}{2(Z+h/2)^{3/2}} \tag{8}$$

The Rabi splitting is clearly due to the interaction between the dipole antenna and the surface phonons and is proportional to the LO-TO splitting δ, i.e. to the square root of the electromagnetic field generated by the surface phonons. It is also a near-field effect since the Rabi splitting rapidly closes up as $(Z+h/2)^{-3/2}$ with increasing separation Z (Fig. 2(b)).

3. Full numerical simulations

In order to go beyond the dipolar approximation used in the analytical model and to take into account the actual shape of the antenna and its polarizability, as well as the plasmon and phonon dampings, we have conducted numerical simulations based on the Green Dyadic Method (GDM) [28, 29]. This method yields exact solutions of Maxwell equations in the frequency domain. The permittivity of gold in the far infrared range has been taken from experimental data [30]. In all the simulations, the thickness of the antenna and its width were set to 100 nm and 200 nm, respectively.

First, the antenna is in contact with the GaN surface in order to maximize the antenna-surface interaction. This configuration is also realistic as it can be achieved experimentally using lithography techniques for instance [31]. The resonance frequencies obtained in this configuration
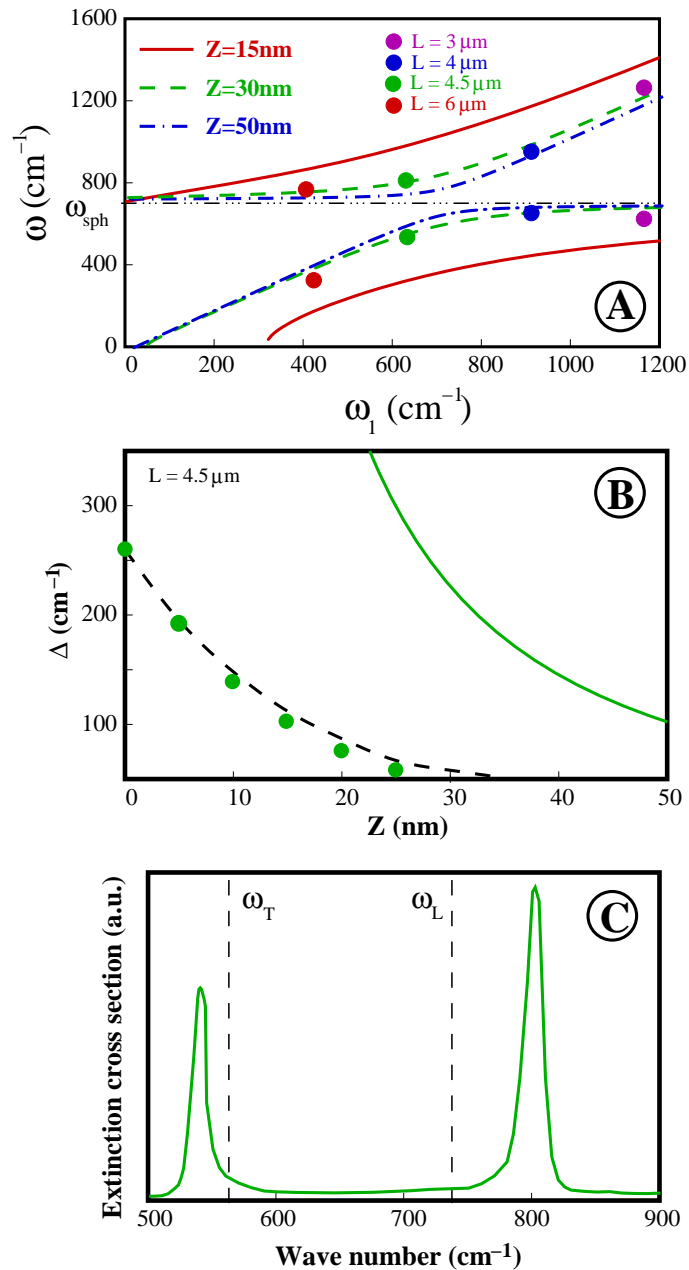
Fig. 2. a. Resonance frequencies ω_+ (upper branches) and ω_- (lower branches) obtained from the analytical model as a function of the dipole antenna frequency ω_1 and for different dipole–to–surface separations Z. The dots are the results of the Green Dyadic Model (GDM) simulations performed for a gold antenna in contact with the GaN surface (Z=0). The antenna length has been changed from 3 to 6 μm (see color code). b. Analytical (full line) and GDM (dots) Rabi splitting Δ as a function of the antenna-to-surface separation. The dashed line is a fit of the GDM results (green dots) with the analytical model (Eq. (8)) using α_0 as an adjustable parameter. c. Extinction spectrum simulated using the GDM for a 4.5 μm antenna located on a GaN substrate.

for different antenna lengths are shown in Fig. 2(a). The strong interaction between the dipolar surface plasmons of the antenna and the surface phonons is corroborated by the numerical simulations : an anti-crossing behavior is observed when the surface plasmon frequency is tuned to the surface phonon frequency. That occurs for an antenna length around 4.5 μm. The two branches in Fig. 2(a) are associated with hybrid surface plasmon-surface phonon excitations hereafter named plasphonic excitations. The extinction spectrum in Fig. 2(c) shows the corresponding Rabi-splitted peaks. The linewidth of these peaks are much smaller than the Rabi splitting, thereby confirming the strong coupling regime. The analytical model overestimates the Rabi splitting because the actual polarizability of gold is smaller than the antenna volume and also because of the finite width of the antenna. Plasmon and phonon dampings also reduce the Rabi splitting. One can notice that a dipole located at Z=30 nm gives nearly the same Rabi splitting as the antenna in-contact with the heteropolar surface.

Second, GDM simulations were performed for various antenna-surface separations. As shown in Fig. 2(b) the Rabi splitting obtained with GDM decreases as $Z^{-3/2}$ in agreement with the analytical model. Moreover, the analytical Rabi splitting (Eq. (8)) has been adjusted to the numerical simulations using the polarisability α_0 as a fitting parameter. To do so, the Z-values of the analytical model were shifted by 30 nm, which corresponds to the equivalent dipole location. The so-obtained polarizability α_0 is 30 % smaller than the antenna volume assumed initially.

To go deeper into the understanding of the surface plasmon-surface phonon hybridization, the electric near-field maps associated to the plasphonic excitations were generated for the strong and weak coupling regimes as well as for the non-interacting situation (Fig. 3).

First, the electric-fields mapped at the frequencies ω_+ = 800 and 740 cm^{-1} of the upper plasphonic branches, exhibit spatial distributions which are typical of dipolar surface plasmons (Figs. 3(a)-3(b)). For the antenna in-contact with the GaN surface (Fig. 3(a)) the Rabi splitting is maximum and the electric near-field enhancement reaches a factor 17 at the antenna ends. With a 20 nm air-gap (Fig. 3(b)), the electric-field enhancement is reduced because of the weaker surface plasmon-surface phonon interaction.

Second, in the case of a non polar semiconductor (δ=0) there are no (electromagnetic) surface phonons. Nevertheless, the surface is still responsible for a dipole image effect which impacts the surface plasmon frequency $\omega_{SP}(Z)$ and the electric field distribution of the gold antenna. To simulate this situation we have removed the polar phonon contribution to the dielectric response which then reduces to $\varepsilon(\omega) = \varepsilon_\infty$ ($\omega_L = \omega_T$ in Eq. (1)). The corresponding near-field distribution is shown in Fig. 3(c). As can be seen, the field enhancement is very weak compared to the strong interaction regime (Fig. 3(a)). This clearly points out the interest of the plasphonic excitations : the strong coupling between polar surface phonons and surface plasmons allows for enhancing the electric near-field amplitude of the gold nano-antenna by nearly one order of magnitude (Figs. 3(a)-3(c)).

Finally, Fig. 3(d) shows the electric-field enhancement mapped inside the GaN at the frequency ω_- = 540 cm^{-1} of the lower plasphonic branch. The near-field distribution is different from the typical dipolar distribution (Fig. 3(a)) and resembles that of a high order Fabry-Perot mode [23]. Such a distribution is not observed in the case of a non polar surface. In fact, because the antenna has a finite length and interacts strongly with the heteropolar surface, the phonon-like plasphonic mode is confined within a region defined by the antenna length L. The wavelengths of such confined modes, labeled by an integer l, are given by

$$\frac{\lambda}{n_{eff}} \cdot (l+1/2) = L \tag{9}$$

where only modes with electric field distributions that are anti-symmetric with respect to the antenna center are considered. This symmetry restriction is imposed by the dipolar surface
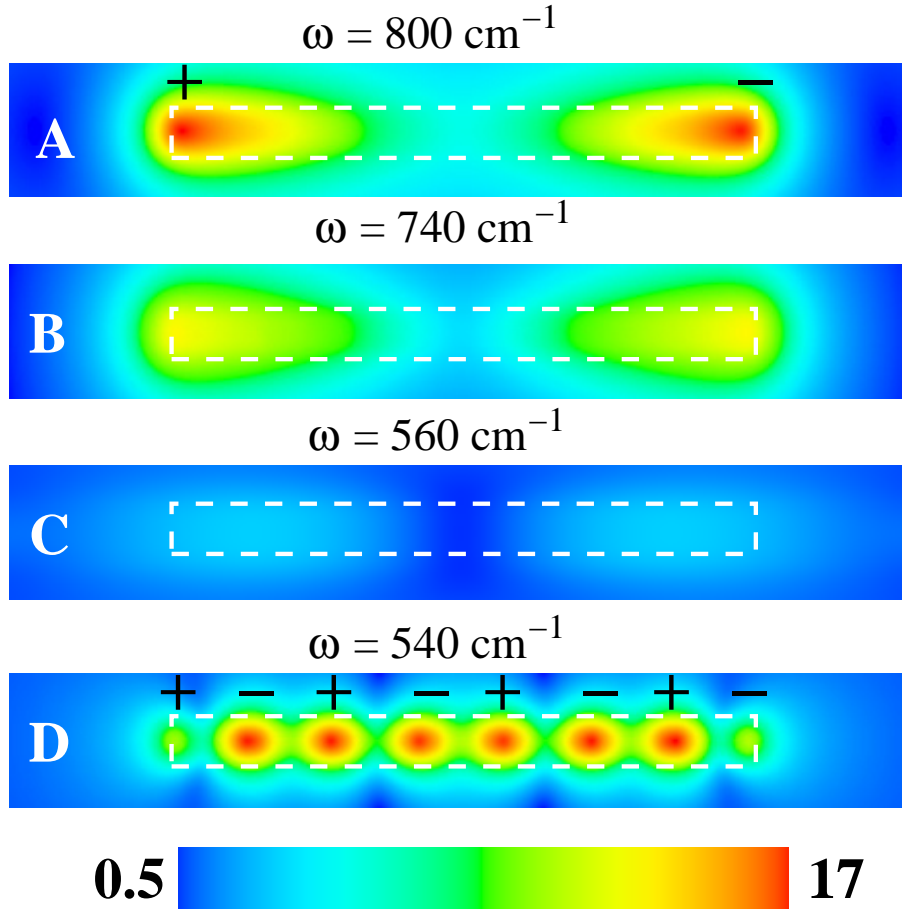
Fig. 3. GDM electric near-field enhancement $|E(r)/E_0|$ maps simulated for a 4.5 μm gold antenna close to either a GaN surface (Figs. 3(a)-3(b)-3(d)) or a non dispersive ($\varepsilon(\omega) = \varepsilon_\infty$) surface (Fig. 3(c)). In Figs. 3(a)-3(c)-3(d) the antenna is in contact with the surface whereas in Fig. 3(b) it is separated from the surface by a 20 nm air-gap. The maps are shown in planes parallel to the surface at 50 nm above the antenna (Figs. 3(a)-3(b)-3(c)) and 50 nm below the GaN surface (Fig. 3(d)). In Figs. 3(a)-3(b)-3(d) the frequency of the incident electric field is resonant with the Rabi-splitted frequencies $\omega_+ = 800$ cm^{-1}, $\omega_+ = 740$ cm^{-1} and $\omega_- = 540$ cm^{-1}. In Fig. 3(c) $|E(r)/E_0|$ is mapped at the surface plasmon frequency $\omega_{SP}(Z=0) = 560$ cm^{-1} in the case of a non polar substrate (δ=0). The sign, in Figs. 3(a)-3(d), of the surface polarisation charge at the field intensity maxima was determined from the GDM simulations.

plasmon of the antenna (Fig. 3(a)) which is anti-symmetric. From Fig. 3(d), one can notice that the antenna is acting as a $7\lambda/(2n_{eff})$ cavity (i.e. $l = 3$). Hence, using a cavity length L = 4.5 μm and $\lambda = 1/\omega_- = 18.5$ μm, one obtains an effective optical index $n_{eff} = 14.4$. This value is larger than the optical index of GaN (around 7.5 at $\omega_- = 540$ cm^{-1}) due to the contribution of the gold antenna. Indeed, in the frame of this simple confinement based assumption, the effective optical index accounts for the interaction between the plasmonic and the phononic excitations.

4. Conclusion

In summary, the hybridization between the surface plasmons of a metallic nano-antenna and the surface phonons of an heteropolar semiconductor has been studied theoretically using both an analytical approach and numerical simulations. This hybridization is governed by the plasmonic and phononic near-fields and may lead to Rabi-splitted plasphonic excitations. It allows a fine tuning of optical resonances and can be exploited for far-infrared based sensing. The mixed character of the plasphonic excitations has also been pointed out from the simulated electric near-field maps. In particular, we found that, in the strong coupling regime, the electric field enhancement at the nano-antenna ends is one order of magnitude larger than the one obtained with a non-polar semiconductor surface. This allows us introducing the concept of *active phonic surface* : the electromagnetic field carried by the surface phonons of an heteropolar semiconductor can be harvested by the metallic antenna via the strong near-field interaction thus leading to additional field enhancement. Plasmonic laser antenna [32] could benefit from active phononic surfaces. Finally, we have reported on a new type of spatial confinement effect which does not make use of band offset, dielectric or mechanical mismatch. The confinement of the phonon-like plasphonic excitations arises because of the strong and spatially localized characters of the plasphonic interaction and is basically a near-field effect.